Biotechnology Reports 29 (2021) e00592

Contents lists available at ScienceDirect

Biotechnology Reports

journal homepage: www.elsevier.com/locate/btre

Production, purification, and process optimization of intracellular pigment from novel psychrotolerant Paenibacillus sp. BPW19

Bhagyashree Padhan, Kasturi Poddar, Debapriya Sarkar, Angana Sarkar*

Department of Biotechnology and Medical Engineering, National Institute of Technology Rourkela, Odisha, 769008, India

ARTICLE INFO

Article history:
Received 31 May 2020
Received in revised form 16 December 2020
Accepted 10 January 2021

Keywords:
Bacterial pigment
Intracellular
Microstructure
Solvent extraction
Chromatography

ABSTRACT

A pink pigment-producing bacterial strain was isolated from wastewater and identified as *Paenibacillus* sp. BPW19. The motile bacterial strain was Gram-positive, acid fermenting, glucose, sucrose utilizing and rod-shaped with an average cell length of 1.55 μm as studied under the Environmental Scanning Electron Microscope. Even though being psychrotolerant, the cell growth condition of BPW19 was optimized as 25 ºC along with pH 8, and 2.25% inoculum concentration considering the operational ease of the production. Sonication assisted solvent extraction produced 5.41% crude pigment which showed zones of exclusion against gram-negative strains *Escherichia coli* DH5α, *Enterobacter* sp. EtK3, and *Klebsiella* sp. SHC1. Gas Chromatography-Mass Spectrometry analysis of the crude pigment exhibited the dominant presence of major compounds as dotriacontane; 3,7 dimethyl 7 octanal; 1-eicosene and erucic acid. While column chromatography (ethanol:chloroform in 1:4 (v/v) ratio) purified pigment was identified as erucic acid using Nuclear Magnetic Resonance with a net yield of 3.06%.

1. Introduction

Pigments and dyes are one of the most utilized supplements used in a wide range of industries including food and beverage, textile, leather, cosmetics, pharmaceuticals, paper, dye-sensitized solar cells, etc. not only to increase the aesthetic of the product but also to improve the taste, quality, and durability of it [1,2]. The demand of the pigments and dyes will see an annual increment of 5% during 2020–2027 from its current market of approximately 33.20 billion US dollars [3]. The post-industrial revolution era experienced a significant increase in market demands of synthetic pigments for their high productivity, high stability, high intensity, low production cost, and varied applications [2]. However, since these pigments directly impact the health and well-being of individuals as well as the environment, they are scrutinized by researchers. Recent reports suggesting the carcinogenic activity of carmoisine or mutagenic activity, allergy, and hyperactivity associated with Tartrazine, Allura Red, Sunset Yellow, and Brilliant blue have made people apprehensive about the use of synthetic pigments and many governments have imposed ban or restrictions on their uses [4]. Apart from these, pigment and dye effluents from various industries like textile, leather, and pharmaceuticals accumulate and contaminate the aquatic environments. For example, approximately 10,000 different synthetic textile dyes are found in industrial effluents that get deposited in the different biosphere as micropollutants [5–8]. Most of these contaminants are non-biodegradable or on degradation produce carcinogenic compounds [7,9]. Management of such contaminants incurs high cost and complexity of the process, and inefficient removal [6,10]. To overcome these hurdles, complex treatment strategies involving nanomaterials have gained interest [11,12]. Nanostructures degrade dyes and particulate contaminants in an eco-friendly and cost-effective way by advanced oxidation processes such as photocatalysis, sonolysis, and Fenton reactions [13–16]. Lately, several nanoparticles [17,18], composites [19], nanocrystals [9,20,21], sorbents [22–24] have been developed and synthesized for the treatment of water contaminated by dyes and other pollutants.

Though these advanced wastewater treatment strategies have been developed to reduce the toxicity of these persistent micropollutants in the environment, these processes have their shortcomings like the requirement of large infrastructure, huge investment, skilled labor, and nanotoxicity [25]. The best possible alternative to protect the environment, as well as human health, should be re-establishing the interest towards the natural pigment and dyes. Natural pigments from plants and minerals have been used from ancient times due to their compatibility, the presence of bioactive compounds, and less toxicity to the environment [26,27].

* Corresponding author.
E-mail addresses: bhagyashreepadhan96@gmail.com (B. Padhan), kasturi.p93@gmail.com (K. Poddar), deb.apn@gmail.com (D. Sarkar), sarkara@nitrkl.ac.in (A. Sarkar).

https://doi.org/10.1016/j.btre.2021.e00592

Recently, researchers have been investigating bacterial pigments as a form of natural pigment which has the potential to meet the existing market demands without inducing toxic effects on the environment [28]. Moreover, pigments extracted from bacteria are more advantageous than other natural sources like plants or minerals as bacteria are easily available and can be cultured in large scale bioreactors, can be engineered and optimized to increase the yield, simple and easy downstream processing, low maintenance and no requirement of large arable lands and labor, unlike plant pigments, for cultivation and processing, utilizes food and agricultural wastes as substrates promoting waste minimization [29]. Since seasonal and geographical variations affect plant growth, it eventually limits the overall pigment production from plant sources. Bacterial pigments on the other hand have no seasonal or geographical limitations. They also contain different biological properties like antioxidants, anti-inflammatory, antifungal, and anti-carcinogenic properties which makes them suitable for the food and pharmaceutical industries [30]. Apart from food and pharmaceuticals, bacterial pigments have application in several fields such as pigment pyocyanin from *Pseudomonas aeruginosa* as textile dye [31], phycocyanin from *Nostoc linckia* for the synthesis of silver nanoparticles [32], prodigiosin from *Serratia marcescens* for the synthesis of dye-sensitized solar cells [33], Violacein from *Chromobacterium violaceum* as immunostimulator with potential to be applied in immune therapies [34] and many others as listed in Table 1 [35–42]. The applicability of bacterial pigment in various industries displays its potential to compete commercially with the existing synthetic pigments in the market. Optimization of bacterial growth conditions such as temperature, pH, incubation time, etc. along with appropriate pigment isolation methods can produce huge quantities of pigment to sustain its commercial usage. Since bacterial pigments can also be intracellular, the loss of the pigment during the extraction and purification process results in a relatively lower net yield of the pigment than other extracellular bacterial pigments or other plant pigments. Hence, the selection of an appropriate extraction method is crucial for obtaining intracellular bacterial pigment. There are several methods used for extraction of intracellular pigment which involves organic solvents, solid-phase extraction, homogenization, freeze-thaw method, ultrasonication, inorganic acids, soxlet method, and others [80]. Amongst all these methods, the solvent extraction method using organic solvents like ethanol and methanol is the simplest and most cost-effective method. These methods can also be used exclusively or in suitable combinations with other methods keeping in view their availability, simplicity, and production cost for higher yields.

To move towards retaining the importance of natural pigment, in this current study bacterial pigment production was investigated. To the best knowledge, the pigment production ability of any strain from the Paenibacillus genus is being reported for the first time. The intracellular pigment production ability of the test strain was evaluated and the chief component of the pigment was also identified along with some characteristic property of the producing strain.

2. Material and methods

2.1. Isolation and identification of pigment-producing bacteria

Wastewater samples collected from the oxidation ponds of Rourkela, India (22.26 °N, 84.85 °E) were spread on Reasoner's2A (R-2A) (M1687, Himedia, USA) agar plates and incubated at 30 °C for 3 days. The pigment-producing colonies of BPW19 were isolated and pure colonies of the strain was obtained by subsequent rounds of quadrant streaking method on sterile agar plates with 1.5 % (w/v) of agar. The strain was further identified by analyzing its 16S rRNA gene [43]. The genomic DNA of the strain was isolated from the cell culture pellet using a standard enzymatic protocol with some modifications along with a Gram-positive control, *Bacillus subtilis,* and a Gram-negative control, *Escherichia coli*. The cell culture was divided into four batches and was primarily subjected to four different types of cell lysis treatment, respectively. The treatment methods include sonication for 30 min; boiling at 100 °C for 15 min; boiling at 100 °C for 10 min followed by sonication for 20 min; alkali lysis using 1 M NaOH for 10 min and adding 1 M HCl to cease the lysis treatment post the incubation period [44].

The genomic DNA was then extracted from the treated cells following the standard enzyme assisted cell disruption procedure followed by solvent extraction using PCI (Phenol:Chloroform: Isoamyl alcohol) in the ratio 25:24:1 and successive purification using ice-cold ethanol. The 16S rRNA gene was particularly amplified with the help of degenerative universal forward primer 27 F and reverse primer 1492R using hot-start PCR (Veriti 96-Well Thermal Cycler, Applied Biosystems, Thermo Fischer Scientific, Singapore) [45]. The amplification of the gene was initiated primarily by denaturing the DNA at 95 °C for 5 min succeeded by 35 complete cycles of the denaturation, annealing, and elongation. Denaturation of the DNA was conducted at 95 °C for 1 min which followed the annealing of the primers with the DNA strands at 52 °C for 50 s and then elongation of the strands for 1.5 min at 72 °C. The final elongation is terminated with an extension of 10 min. The PCR amplified product was purified using a gel extraction kit (Genetix Biotech Asia Pvt Ltd, New Delhi, India) and Sanger sequencing was performed from Eurofins Genomics India Pvt Ltd, Bangalore, India [46]. The obtained sequence was edited using BioEdit (v7.0.5) software to remove terminal noise response during the sequencing. Further, BLASTN (Basic Local Alignment Search Tool for Nucleotide) was performed on the edited sequence using NCBI (National Centre for Biotechnology Information) database to identify the related strains having homologous or identical sequences. The identified homologous strains were aligned by multiple sequence alignment CLUSTALW using MEGA7 software. From this multiple alignment result, the final phylogenetic tree

Table 1
Isolated pigments from different bacterial species.

No.	Bacterial species	Source	Pigment	Application	Reference
1.	*Serratia marcescens*	American type culture collection	Prodigiosin	Fabric dye	[35]
2.	*Chryseobacterium artocarpi*	Orchard soil	Flexirubin		[36]
3.	*Streptomyces coelicoflavus*	Soil	Red pigment	Anthracyclines analog	[37]
4.	*Chryseobacterium* sp. and *Hymenobacter* sp.	Soil	Xanthophylls	Dye-sensitized solar cells	[38]
5.	*Brevundimonas* sp.	Marine water	Astaxanthin		[39]
6.	*Lysobacter oligotrophicus*	Freshwater, Antarctic	Melanin	Removal of free radicals and ROS	[40]
7.	*Pseudomonas* spp.	Dairy product	Phycoerythrobilin		[41]
8.	*Xanthomonas* sp.	Marine soil	Yellow	Fabric dye	[42]
	Sarcina sp.		Orange		
	Rhodotorula sp.		Pink Red		

was constructed using the bootstrap method by the neighbor-joining algorithm in MEGA7 software. For the construction of the phylogenetic tree, an out-group was considered as *Staphylococcus aureus* df5 (LN929744) [47–49].

2.2. Characterization of isolated strains

2.2.1. Chemical characterization

The molecular setup of the cell wall of the isolated strain was characterized by the Gram staining method using Gram Staining Kit (K001, Himedia, Mumbai, India). The metabolic biochemical characterization of the isolated bacterial strain was performed by the IMViC test which includes four different examinations, viz. Indole production test, Methyl red test, Voges-Proskauer test, and Citrate utilization test using IMViC Identification Kit (207900011, Microxpress, Goa, India). The carbohydrate utilization profile of the isolated bacterial strain was performed using different carbohydrate-containing media provided in the same kit [50]. All the biochemical characterization experiments were validated using two model organisms viz. *B. subtilis* and *E. coli.*

2.2.2. Physical characterization

A motility test was performed by the hanging drop method using a circular concavity slide. In a clean glass slide, a single drop of overnight grown culture was placed by micropipette and covered with a concavity slide using petroleum jelly without disturbing the drop. The slide was flipped carefully and the drop was observed under a total of 1000X resolution in a compound microscope to identify any motion inside the hanging drop [51]. To validate the process, *B. subtilis* was used as a positive control and *Klebsiella pneumonia* as a negative control.

The isolated bacteria were further physically characterized by Environmental Scanning Electron Microscope (ESEM). Sample preparation steps include fixation by 2.5 %–3 % glutaraldehyde in phosphate buffer at room temperature for 1−2 h followed by washing in phosphate buffer for 10 min. Post-fixation was done by using 1 %–2 % osmium tetroxide in phosphate buffer for 1−2 h followed by washing in distilled water for 10 min. Next dehydration at different ethanol concentration of 30 %, 40 %, 50 %, 60 %, 70 %, 80 %, 90 % for 10 min at each concentration and dehydration at 100 % ethanol for twice for 20 min. The specimen was then dried and mounted on carbon tape and the sample was viewed under the Environmental Scanning Electron Microscope (ESEM) (Quanta 600 FEG, FEI, Japan) [52]. Moreover, the effect of temperature on bacterial growth was studied for a declining temperature range of 35 °C to 5 °C to evaluate the psychrotolerant nature of the isolated strain.

2.3. Optimization of pigment production

To optimize the biomass production and cellular growth of the isolated strain BPW19, a two-level, three factorial central composite design (CCD) was obtained using Design-Expert software (Trial version). For the biomass production, the three main contributing factors were taken as the incubation temperature, pH and inoculum percentage which are represented as coded values of A, B, and C, respectively [43,53]. The levels for A, B, and C were considered as 25 °C and 37 °C, 6 and 8, 1.5, and 3.5, respectively. A total of 20 run combinations were proposed by the software to obtain the responses of biomass production. For each run, 150 mL of culture was performed in constant shaking of 140 rpm and incubated for 4 days [54].

Analysis of variance (ANOVA) was used to test the effect of different factors on response variables and interaction between the response and the interaction variables were examined using model equations. Error sum of square (SSE), regression sum of square (SSR) and corrected sum of squares (SST) was determined using ANOVA analysis. Fisher's F-test checked the statistical significance of the model whereas the coefficient of determination R^2 expressed the polynomial model's fit quality. Based on the effect of three factors, the respective contour plots were obtained for both the levels [55,56].

2.4. Bacterial cell harvesting using lab-scale bioreactor

To obtain biomass for pigment production, the isolated bacterial strain was cultured in a total of 2.5 L of R-2A broth in a stirred tank bioreactor (BIOSTAT B plus, Sartorius Stedim Biotech, Germany) constantly maintaining the optimized culture conditions for 4 days in presence of constant shaking of 140 rpm at 25 ºC. After the incubation time, the color of the broth was found to be changed to pink. From the broth, the biomass was harvested using centrifugation (5430R, Eppendorf, Germany) at 7000 rpm at room temperature for 15 min. The pellet of the collected biomass from the 2.5 L culture was dried in open air overnight and weighed [57].

2.5. Pigment extraction, purification and yield analysis

The pigment extraction process was initiated by dissolving the whole of the harvested biomass in 50 mL of 100 % methanol (v/v) assisted by vortexing to confirm a homogenous solution. The pigment appeared to be inside the cell as the centrifuged broth exhibited no extraction of the produced pigment. Hence the pigment was concluded to be intracellular. The dissolved cells of isolated bacterial strains were then lysed by ultrasonication treatment in a bath sonicator (Digital Ultrasonic Cleaner LCMU-2, Labman Scientific Instruments, Chennai, India) for 30 min. After sonication, the solution mixture was centrifuged at 7000 rpm at room temperature for 15 min to obtain a colorless pellet and colored supernatant [26,58]. This methanol solution along with the extracted pigment was then air-dried for 3 days in a dust-free environment. After drying, the extracted crude pigment was weighed.

The purification of the crude pigment was performed by Column Chromatography assisted with Thin Layer Chromatography (TLC). Initially, a homogenous mixture of dried crude pigment and silica were prepared and column chromatography was performed using dissolved Silica Gel G (GRM7480, Himedia, New Delhi, India) in chloroform in 1:4 (w/v) ratio. The fractions were eluted using a solvent mixture of ethanol:chloroform in 1:4 (v/v) ratio [59,60]. Each eluted fractions were examined by TLC analysis in pre-coated TLC plates (TLC Silica Gel 60 F_{254}, Merck, India) using the same solvent as the mobile phase for examining the purity of the fractions. For each TLC run, the retention factor (R_f) value was calculated by Eq. (1) [27].

R_f= Distance traversed by the pigment/Distance traversed by the solvent (1)

Elute showing single mobile front having identical R_f value was considered as a single component. Such fractions were cumulated and the solvent was evaporated to obtain the purified dried component. From the obtained data, stoichiometric equations were produced to represent each of the steps and net yield was calculated.

2.6. Antibacterial assay

The antibacterial effect of the crude pigment was studied by inoculating it with different Gram-positive and Gram-negative bacterial strains on Luria Bertani (LB) (M575) (Himedia, India) agar media plates. The Gram-negative test organisms include *Escherichia coli* DH5α, *Enterobacter* sp. EtK3, *Klebsiella* sp. SHC1,

whereas Gram-positive test strain includes *Bacillus subtilis* MTCC 2616. Young suspension cultures of the test strains were spread over in different sterile LB agar plates. Paper discs of mm diameter impregnated with 5 μL of the pigment suspended in a solvent were placed on the plates and incubated at 30 °C for 3 days. A parallel plate was maintained by using a similar paper disc impregnated with only methanol as a control for the experimental condition. Proper radial diffusion of the pigment was allowed by keeping the plates upright in an undisturbed condition [27,61].

2.7. GC–MS analysis

For the Gas Chromatography-Mass Spectrometry analysis of the crude pigment, a pinch of dried crude pigment was dissolved in 500 μL of methanol. The sample was analyzed using Gas Chromatography (7890B, Agilent Technologies, United States) using standard HP-5-MS column (7890B, Agilent Technologies, United States) and the compounds were detected by Mass Spectrometer (5977A, Agilent Technologies, United States). The initial temperature of the gas chromatography was maintained at 50 °C and for 1 min and escalated up to 180 °C at a rate of 20 °C/min and held for 0.5 min. The temperature was increased again at a rate of 20 °C/min up to 280 °C and held for 3 min. A split ratio of 1:50 was maintained with Helium being used as inert carrier gas at a flow rate of 1 mL/min [56,62,63].

2.8. NMR analysis of pigment compound

The characterization of the purified pigment was performed by Nuclear Magnetic Resonance (NMR) Spectroscopy. A pinch of dried purified pigment was dissolved in 500 μL of deuterated dimethyl sulfoxide (DMSO) (DLM-10-S-10 mL, Cambridge Isotope Laboratories Inc, United States) and the solution was made homogenous [64]. The mixture was then analyzed in 400 ultrashield NMR (Avance III, Bruker, United States) to evaluate the number of protons (^{1}H) at 500.13 MHz and carbon (^{13}C) at 125.77 MHz frequency [61].

2.9. Statistical analysis

The experiments were performed in triplicates and the obtained results were statistically analyzed in Origin Pro (v11.0) using Analysis of Variance (ANOVA) test. The significant difference was calculated statistically using the Chi-Square test.

2.10. Nucleotide sequence accession number

The obtained sequence has been submitted to the GenBank database of the NCBI with an accession number of MK944323.

3. Results and discussion

3.1. Phylogenetic analysis of bacterial strain

The pink-colored colony was collected from the wastewater spread plates and streaked multiple times to screen out the pure strain. DNA extraction of the bacterial strain using enzymatic cell lysis found no yield of genomic DNA, while both the control microbes showed a significant yield of genomic DNA following the same protocol. This indicated high resistivity of the isolated bacterial cell wall towards cell lysis due to its complex cell wall composition. The DNA extraction was successful only after a more vigorous cell lysis approach like sonication or boiling combined with sonication.

BLASTN analysis of the partial sequence of the 16S rRNA gene of BPW19 confirms the relation of the isolated strain to different species of *Paenibacillaceae* family. The phylogenetic analysis showed that *Paenibacillus taichungensis* BCRC 17757 (EU179327) had the most resemblance with BPW19 (MK944323) (Fig. 1). Other closely related bacterial strains were found to be *P. oceanisediminis* L10 (NR118217), *P. dongdonensis* KUDC0114 (KF425513), *P. panacisoli* 1411 (AB245384), and *P. terrae* AM141 (AF391124). This confirmed the relation of the isolated BPW19 with *Paenibacillaceae* family and established it as a member of the family. *Paenibacillaceae* family is well known as a soil bacteria and associated with the growth of different plants like maize, cucumber, rice, pumpkin, etc.

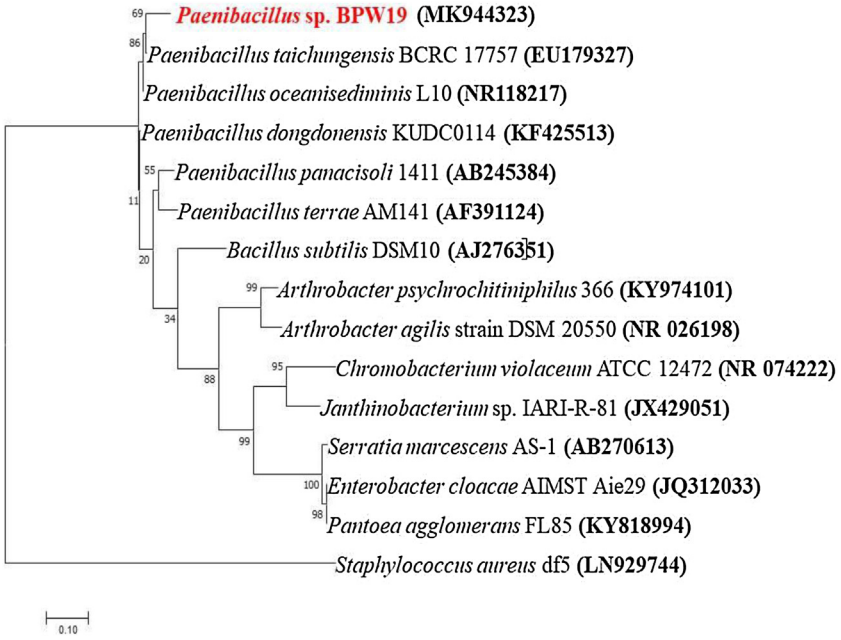

Fig. 1. Phylogenetic tree analysis of the isolated strain BPW19 (MK944323).

showing abilities like nitrogen fixation, phosphate solubilization and iron acquisition [64,65]. Even biocontrol and insecticidal effects along with antimicrobial effects were also observed by members of the *Paenibacillaceae* family [64]. Although no *Paenibacillaceae* family members have been reported in pigment production to date. The phylogenetic analysis also showed that the isolated strain BPW19 is distantly related to *Bacillus subtilis* and other well-known pigment-producing bacteria like *Serratia marcescens, Enterobacter cloacae, Chromobacterium violaceum,* and *Arthrobacter agilis*. *Staphylococcus aureus* was considered as an outgroup to construct the phylogenetic tree.

3.2. Characterization of strain

The Gram staining differentiates bacterial strains based on their cell wall content: Gram-negative strain containing lower polysaccharide and higher lipid percentage hence staining red by safranin, characterizing less rigid cell wall, and Gram-positive strain having higher polysaccharide and lower lipid content hence staining purple by crystal violet signifying the presence of rigid cell wall. The strain BPW19 was observed to be Gram-positive and rod-shaped characterizing its rigid cell wall which was evident during the cell lysis process of DNA extraction. During the experiment, a Gram-positive control, *B. subtilis,* and a Gram-negative control, *E. coli* was maintained to validate the result.

The ability of the bacterial strain to convert tryptophan into indole was evaluated by the Indole test in which Kovac reagent turns to pinkish-red from colorless in presence of indole. The strain BPW19 did not show any such changes in the color signifying its inability to produce indole fro tryptophan. For this analysis, *E. coli* was considered as a positive control, and *B. subtilis* was considered as a negative control. The acid fermentation ability of the isolated strain BPW19 was examined by methyl red test in which the media contained a pH indicator (methyl red) which turns yellow to red in the periphery of a bacterial colony producing acid. BPW19 exhibited similar changes indicating acid fermentation ability. *E. coli* and *B. subtilis* were maintained as a positive and negative control, respectively. The Voges-Proskauer test was used to check the utilization 2,3 butanediol pathway to produce acetoin from glucose by the bacterial strain in which the test reagent containing α-naphthol and potassium hydroxide turns pinkish for a positive result and remain colorless or turns slightly copper for the negative result. The negative results for BPW19 in the Voges-Proskauer test confirmed that the strain cannot produce acetoin by glucose fermentation. *B. subtilis* and *E. coli* were considered as a positive and negative control, respectively for the examination. The citric acid test was conducted to confirm the citrate utilization ability of the bacterial strain as a sole carbon source in which a pH indicator turns blue from green due to the increase in the pH of the media as citrate gets depleted. No such color changes of the inoculated citrate media were evident in presence of BPW19 which inferred the inability of the strain to utilize citrate as sole carbon source. *B. subtilis* and *E. coli* were considered as positive and negative control, respectively for the analysis. Carbohydrate utilization profile of the isolated strain BPW19 was constructed following the standard protocol. In the process, the carbohydrate utilization activity generally reduces the pH of the medium due to the production of acids like pyruvic acid and other secondary metabolites. This change in the pH was detected by pH indicator phenol red which turns purple-red to yellow in lower pH. Different carbohydrate was considered and it was found that BPW19 was able to utilize glucose and sucrose as sole carbon sources. While the medium containing carbohydrates like adonitol, arabinose, lactose, sorbitol, mannitol, and rhamnose did not show any changes signifying the inability of the strain to utilize these carbohydrates as sole carbon sources. As a reference carbohydrate profile and validation of the experiment, *B. subtilis* and *E. coli* were considered. The comparative biochemical profile of BPW19 had been represented in Table 2 along with the model organisms *B. subtilis* and *E. coli*.

The strain BPW19 appeared motile when observed under 1000X microscopic magnification which states a character for strains of *Paenibacillaceae* family [66]. *B subtilis* was found motile whereas *K. pneumoniae* was found to be non-motile which ensured the correctness of the experiment. BPW19 appeared rod-shaped with an average cell length of 1.55 μm and was found to have a rough appearance on the cell surface when visualized under 50,000X magnification of the ESEM (Fig. 2). The obtained cell length of BPW19 is smaller than other reported bacterial strains from the *Paenibacillaceae* family, for example, *Paenibacillus dongdonensis*, was reported with an average length of 2.8 μm [67]. On the other hand, BPW19 had larger cell length than bacteria like *S. aureus* which had been reported with an average cell length of 1 μm [68].

3.3. Psychrotolerant nature of BPW19

The bacterial strain was found to grow better in lower temperatures and the cellular growth was observed to be the maximum at 5 °C which is 11.80 % higher than that observed at 25 °C, 60.5 % higher than the growth at 30 °C and almost 296.46 % higher than the growth obtained at 35 °C (Fig. 3). However, the specific growth rate was observed to be more at a higher temperature of 30 °C with 1.64/hr as compared to a lower temperature of 5 °C with 0.66/hr. The cell growth rate at a lower temperature was unsurprisingly lower as the metabolic activities tend to slow down at low temperatures. Since the log phase was more prolonged at lower temperatures, the overall cell growth was obtained higher despite having a lower growth rate. Since BPW19

Table 2
Biochemical characterization of the isolated bacterial strain *Paenibacillus* sp. BPW19.

Biochemical test	Positive	Negative	*E. coli* (DH5α)	*B. subtilis* (MTCC 2616)	BPW19
Gram staining	Violet	Red	–	+	+
Indole test	Reddish pink	Colorless	+	–	–
Methyl red test	Red	Yellowish orange	+	–	+
Voges Praskeur test	Pinkish red	Colorless	–	+	–
Citrate utilization test	Blue	Green	–	+	–
Glucose	Yellow	Red	+	+	+
Adonitol	Yellow	Red	–	–	–
Arabinose	Yellow	Red	+	+	–
Lactose	Yellow	Red	+	–	–
Sorbitol	Yellow	Red	+	+	–
Mannitol	Yellow	Red	+	+	–
Rhamnose	Yellow	Red	+	–	–
Sucrose	Yellow	Red	–	+	+

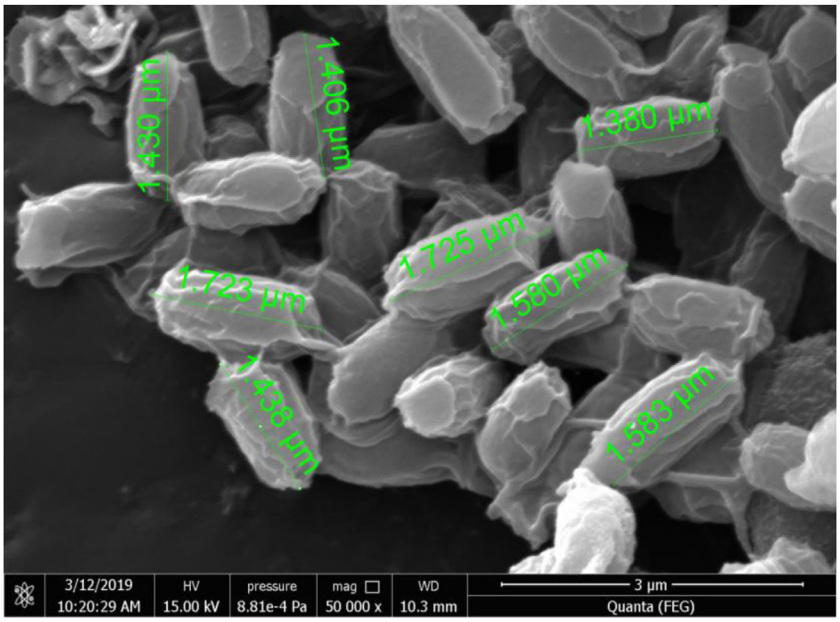

Fig. 2. Visualization of the isolated strain BPW19 under ESEM at 50000X magnification.

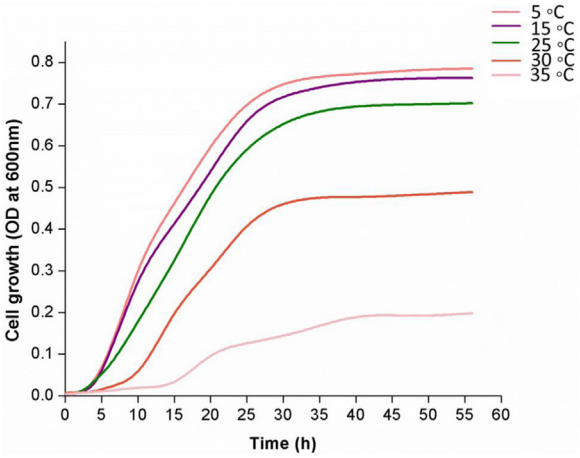

Fig. 3. The effect of temperature on cellular growth of BPW19 indicating the psychrotolerant nature of it.

was able to grow in a temperature range of 5 °C–35 °C it could be considered as a psychrotolerant bacteria [69]. Different strains of *Paenibacillus* had already been reported to be psychrophilic growing at extremely low-temperature conditions. Strains of *Paenibacillus* were isolated from the active permafrost layer of Alaska while another strain from the same family was isolated from chilled ready to eat meals and could sustain lower temperatures of about 7 °C [69–71]. Some other strains were also isolated from soil with their ability to grow at temperatures between 4 °C and 25 °C which is comparable with the isolated strain of the study BPW19 which also exhibits similar temperature range for effective growth [72].

3.4. Biomass production optimization

Based on CCD modeling, a total of 20 runs of the different combination was suggested by the software. The obtained biomass along with the run combinations have been represented in Table 3. The cubic model suggested by the software for cell growth was represented by Eq. (2). The difference between the adjusted and predicted R^2 value was obtained as 0.0451 which is less than 0.2 and the overall R^2 value was determined as 0.9874. These statistics signified the good fit of the model. The ANOVA analysis (Tables 4 and 5) also suggested the model is signified with considerable F and p values and lack of fit was also found non-significant [43].

$$\text{Biomass} = 0.0951 - 0.0006A + 0.0056B + 0.014C - 0.0177AB - 0.0055AC + 0.0013BC + 0.0162A^2 + 0.0043B^2 - 0.0052C^2 - 0.005ABC + 0.0396A^2B - 0.0252A^2C - 0.0232AB^2 \quad (2)$$

where A, B, and C are temperature, pH, and inoculum percentage, respectively.

The model suggested that the pH and inoculum percentage had a positive impact whereas temperature had a negative impact on cellular growth (Fig. 4). According to the model, the preference of low temperature was found collinear with the psychrophilic character of PW19. But maintaining a lower temperature in the bioreactor makes the whole process exothermic but to support that refrigeration would be required [73]. Hence maintaining such low temperatures for industrial production will require energy consumption and incur operational and maintenance costs. The increased amount of biomass obtained at low temperature may not be sufficient to support the elevated process cost. Moreover, a low-temperature process is well known for slow bacterial growth rate, even for psychrophilic bacteria [74]. Hence lowering the temperature will increase operation time to obtain the maximum cell growth which is also not accepted in industrial-scale processes. So the optimum temperature was considered 25 °C which was found sufficient to support cell growth. The acceptance of the model was tested by the run suggested by the software with temperature 25 °C, pH 8, and inoculum percentage of 2.25 %. The predicted value of biomass was 0.19 g. The experimental result obtained was 0.18 g which confirmed the difference between the predicted and experimental value is only 5.85 % which is significantly low.

3.5. Pigment purification and yield

After the sonication process, the intracellular pigment was dissolved completely in methanol. The solution was further considered for TLC analysis which revealed two different bands using a mobile phase of ethanol and chloroform in 1:4 (v/v)

Table 3
Experimental run combination of different process parameters for biomass production optimization of *Paenibacillus* sp. following CCD.

No.	Temperature (ºC)	pH	Inoculum percentage (%)	Response : Biomass (g/L)
1	25	8	3.5	0.19
2	31	7	2.5	0.10
3	37	6	3.5	0.06
4	31	7	2.5	0.08
5	37	6	1.5	0.08
6	41.09	7	2.5	0.14
7	37	8	1.5	0.12
8	25	6	1.5	0.09
9	31	7	2.5	0.10
10	20.91	7	2.5	0.14
11	31	7	4.18	0.10
12	31	7	2.5	0.09
13	25	6	3.5	0.07
14	31	7	0.82	0.06
15	25	8	1.5	0.19
16	31	5.32	2.5	0.12
17	31	7	2.5	0.10
18	37	8	3.5	0.08
19	31	8.68	2.5	0.10
20	31	7	2.5	0.10

Table 4
ANOVA analysis obtained from the model suggested by software for the optimization of pigment production.

Source	Sum of Squares	df	Mean Square	F-value	p-value	
Model	0.0236	13	0.0018	36.12	0.0001	Significant
A-Temperature	2.000E-06	1	2.000E-06	0.0397	0.8486	
B-pH	0.0002	1	0.0002	3.58	0.1072	
C-Inoculum	0.0011	1	0.0011	21.93	0.0034	
AB	0.0025	1	0.0025	50.05	0.0004	
AC	0.0002	1	0.0002	4.81	0.0709	
BC	0.0000	1	0.0000	0.2482	0.6361	
A^2	0.0038	1	0.0038	74.83	0.0001	
B^2	0.0003	1	0.0003	5.36	0.0599	
C^2	0.0004	1	0.0004	7.80	0.0315	
ABC	0.0002	1	0.0002	3.97	0.0933	
A^2B	0.0052	1	0.0052	103.44	< 0.0001	
A^2C	0.0021	1	0.0021	41.86	0.0006	
AB^2	0.0018	1	0.0018	35.28	0.0010	
AC^2	0.0000	0				
B^2C	0.0000	0				
BC^2	0.0000	0				
A^3	0.0000	0				
B^3	0.0000	0				
C^3	0.0000	0				
Residual	0.0003	6	0.0001			
Lack of Fit	7.325E-06	1	7.325E-06	0.1242	0.7389	not significant
Pure Error	0.0003	5	0.0001			
Cor Total	0.0239	19				

Table 5
Fit statistics of the model suggested for optimization of pigment production.

Std. Dev.	0.0071	R^2	0.99
Mean	0.11	Adjusted R^2	0.96
C.V. %	6.72	Predicted R^2	0.92
		Adeq Precision	21.82

signifying the presence of two different chemicals in the crude pigment. The major pink band was observed to have an R_f value of 0.92, where the solvent front was 1.9 cm and the pigment front was 1.75 cm at around 30 °C. The purified pigment was obtained through column chromatography after collecting elutes of the major band considering similar R_f values and dried for further confirmatory analysis.

After 4 days of incubation in bioreactor maintaining the optimized culture conditions, 2.5 L of cell culture broth produced around 3.14 g of dry cell mass. Considering R-2A broth contains 2.36 g/L of carbohydrates and 0.17 g/L of ammonia (a simplest representable form of nitrogen source) the stoichiometric equation, Eq. (3) was produced taking 1 L basis to represent biomass production during the process.

$$2.35\ \text{g carbohydrates} + 0.01\ NH_3 \rightarrow 0.051\ CH_{1.79}O_{0.5}N_{0.2} + 1.117\ \text{g residual} \quad (3)$$

Where $CH_{1.79}O_{0.5}N_{0.2}$ is a universal bacterial biomass representation [43].

This inferred a net biomass yield of 0.35 g of dry biomass/g of carbohydrate. From the obtained 3.14 g of biomass, 0.17 g of crude pigment was recovered following the solvent extraction process. This indicated that the crude pigment was 5.41 % of the biomass by proportion. This solvent extraction process can be represented by the stoichiometric equation, Eq. (4) which was also prepared considering a 1 L basis.

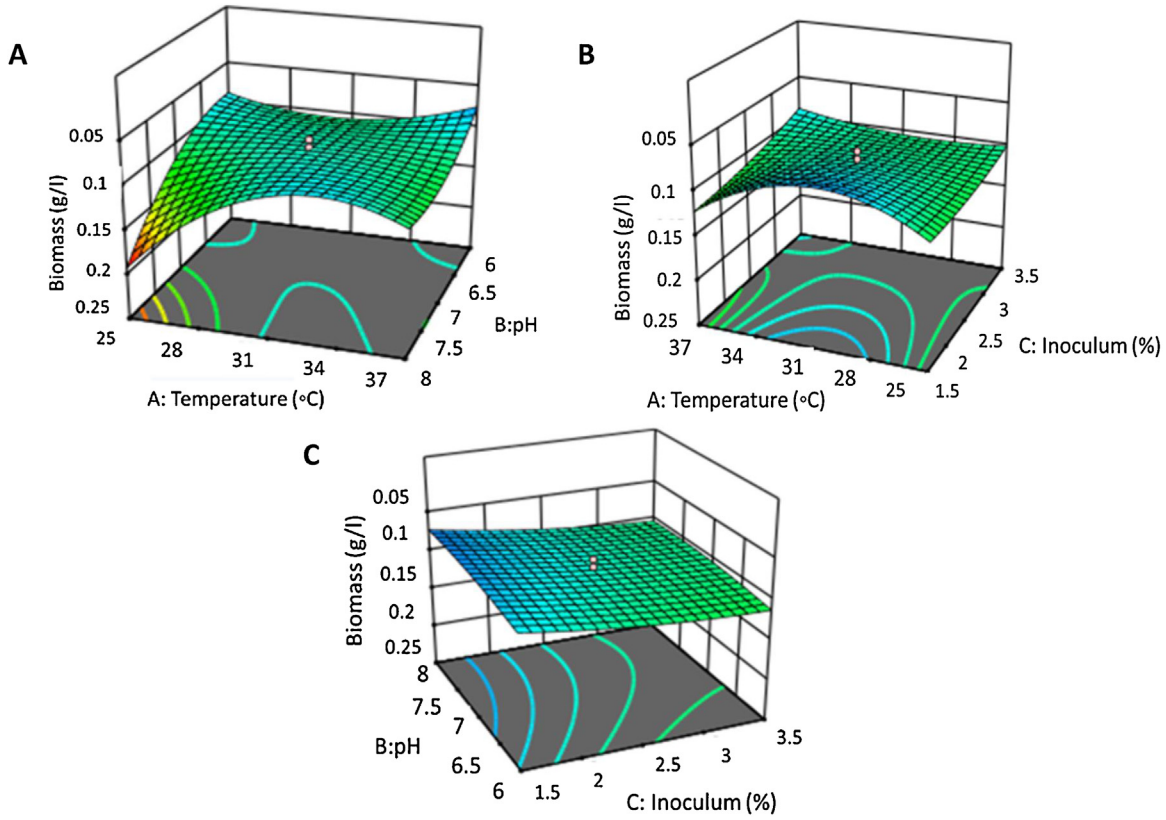

Fig. 4. Contour Plots of interaction between three factors considered during optimisation Temperature, pH and Inoculum (%); (A) Interaction between temperature and pH; (B) Interaction between temperature and inoculum % ; (C) Interaction between pH and inoculum %.

0.051 $CH_{1.79}O_{0.5}N_{0.2}$ → 0.066 g crude pigment + 1.186 g cell debris (4)

The obtained crude pigment was further purified using column chromatography and around 0.1 g of purified pigment compounds was obtained from 0.17 g of crude pigment. This resulted in 57.80 % of the crude pigment if purified as the final pigment compound. This purification process can be expressed stoichiometrically as Eq. (5). The net yield of purified pigment was 3.06 % from biomass.

0.07 g crude pigment → 0.03 g purified pigments + 0.03 g contaminants (5)

The net yield of purified pigment for this process was obtained as 0.1 g from 2.5 L of bacterial culture. The yield obtained for the pigment in this study is comparable with yields reported in recent literature for intracellular pigment isolation from bacteria. The recorded yield in this study was 68 mg/L of crude pigment from the BPW19 strain by the solvent extraction method. This result is 3.5 times higher than the yield of 18.90 mg/L reported for a strain of *D. violaceinigra* [79] and 4.5 times higher than the yield of 15 mg/L reported for *Formosa* sp. [88]. The optimization of process conditions for maximum biomass production led to the higher yield in our study as compared to the other reports. In another report, violacein pigment was produced by *Janthinobacterium* species and optimization of growth conditions was done followed by pigment isolation using solvent extraction method [78]. The obtained yield in the report was 77 mg/L which is comparable with the yield results of the current study.

The higher yield observed in our study was due to the pigment extraction after optimizing the parameters for maximum biomass production followed by the use of only a single-step purification process of the crude pigment. Therefore the production and extraction of the intracellular pigments from BPW19 through solvent extraction provided a higher yield with no energy consumption as compared to other extraction processes, making it a cost-effective approach. Another study on the extraction of intracellular yellow pigment from coral-associated bacteria *Vibrio owensii* TNKJ.CR.24–7 reported a yield of about 1.14 % when isolated with 1-butanol which was comparable with BPW19 strain of this study provided a yield of 3.06 % after purification stating a

Table 6
Comparative representation of pigment yield from other bacterial sources.

Pigment	Type	Species	Pigment isolation method	Yield	References
Indochrome type blue pigment	Extracellular	*Pseudarthrobacter* sp.	Solid-phase extraction	2.5 g/L	[41]
Carotenoid like pigment	Intracellular	*Arthrobacter* sp.	Solvent extraction	0.84 g/L	[77]
Violacein	Intracellular	*Janthinobacterium* sp.	Solvent extraction	77 mg/L crude	[78]
Violacein	Intracellular	*Duganella violaceinigra* str. NI28	Solvent extraction	18.9 mg/L crude	[79]
Prodigiosin	Intracellular	*Serratia marcescens*	Ultrasonication	2.54 ± 0.41 mg/mL	[80]
			Freeze-thawing	0.06 ± 0.02 mg/mL	
			Homogenization	0.49 ± 0.10 mg/mL	
Pink pigment	Intracellular	*Paenibacillus* sp.	Solvent extraction	3.06 g/100 g of biomass	This study

relatively higher yield [76]. Comparative representation of the pigment yield of this study along with other recent works had been discussed in Table 6 [41,77–80].

3.6. Antibacterial assay of crude pigment

The solvent extraction process produced crude pigment which was further evaluated for its antibacterial property. The crude pigment showed antibacterial property against Gram-negative test strains. Growth inhibition zone of about 2.5 mm was obtained against *E. coli* whereas 3.1 mm and 2.9 mm were observed against *Enterobacter* sp. and *Klebsiella* sp., respectively. No antibacterial effect was observed against the Gram-positive bacteria *B. subtilis.* Hence the pigment was found to be effective against Gram-negative bacterial strains. Some reported bacterial pigments exhibited similar kinds of antibacterial activity which include prodigiosin produced by *Serratia* sp. PDGS 120915, phyocyanin pigment by *Pseudomonas aeruginosa*, etc [31,75]. Although no strain of *Paenibacillus* genus was reported with pigment production, however, some strains like *Paenibacillus polymyxa* and *Paenibacillus thiaminolyticus* were reported to produce antimicrobial substances comprised of bacteriocins, lipopeptides, enzymes, and different volatile organic compounds [81].

3.7. GC–MS and NMR analysis

The GC–MS analysis of crude pigment indicated the presence of a variety of complex components (Fig. 5a). Among them, the main four dominating compounds were identified as dotriacontane (16.72 min), 3,7 dimethyl 7 octanal (16.83 min), 1-eicosene (17.17 min) and erucic acid (17.19 min) with percentage area of 1.39 %, 23.66 %, 22.87 %, and 12.75 %, respectively (Fig. 5b). Among these identified compounds, dotriacontane is a long chain hydrocarbon having 32 carbon atoms. It had been reported with antibacterial, antioxidant, and antispasmodic activity. On the other hand, compound 1-eicosene is a suitable anticancer agent and possesses immunosuppressive activity. It also acts as a radical scavenger to reduce the chemical stress.

NMR spectrum analysis was used to identify the component in the purified pigment compound. The ^{13}C analysis confirms the presence of 1 carbonyl compound, two double-bonded carbons (sp^2), and 20 other (sp^3) carbons (Fig. 6a). Proton count also confirmed the presence of a carboxyl group, an internal double bond, and a total of forty-two hydrogen (Fig. 6b). The NMR spectrum analysis combined with the GC—MS report, the component of the purified pigment was identified as erucic acid (Fig. 7). Erucic acid is effectively used as a surfactant in various oleochemical industries and is one of the fundamental compounds in hydraulic fluids [82]. It is also used for the production of lubricants, detergents, plastics, resins, and lacquers [83]. The application of high erucic acid contained oil as cutting oil for metals paves finds its utilization in the metallurgical industries [84].

4. Application of the present work

Pigment production from bacterial sources is beneficial in terms of large scale production with low generation time and presence of different biological compounds like antioxidants and antimicrobials along with biocompatibility, less toxicity, economic and eco-friendly. The present work reported pigment production from a strain of the *Paenibacillus* genus for the first time. The intracellular pigment was extracted using solvent extraction after sonication and heat mediated cell disruption. The solvent extraction process aids in a less expensive pigment production with no energy requirement. Bacterial pigment allows very little amounts of waste generation and also reduces the cost of chief substrates for the production line. The purified compound from the pigment was identified as erucic acid which has its application in oleochemical industries as surfactants and also used in the production of lubricants, detergents, plastics, resins, and lacquers [83]. The compound is also regarded as essential in the metallurgical industries as high erucic acid contained oil is used as cutting oil for metal paves [84]. It is also one of the major compounds used in hydraulic fluids and is considered important in the automobile industries [82]. Other natural sources of erucic acid

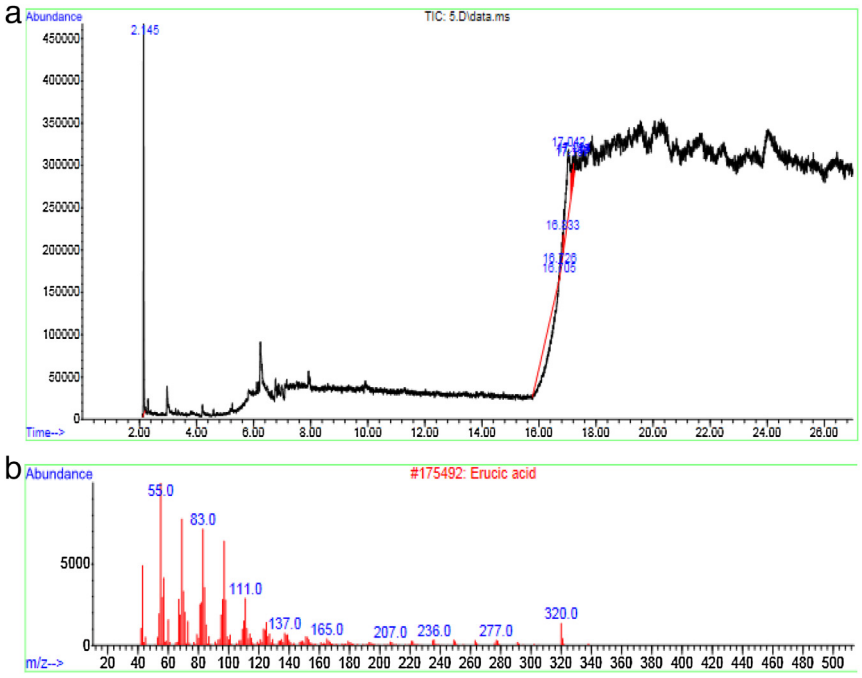

Fig. 5. a The GC–MS chromatogram of the crude pigment. b The GC–MS chromatogram showing the presence of erucic acid as one of the compounds in the crude pigment.

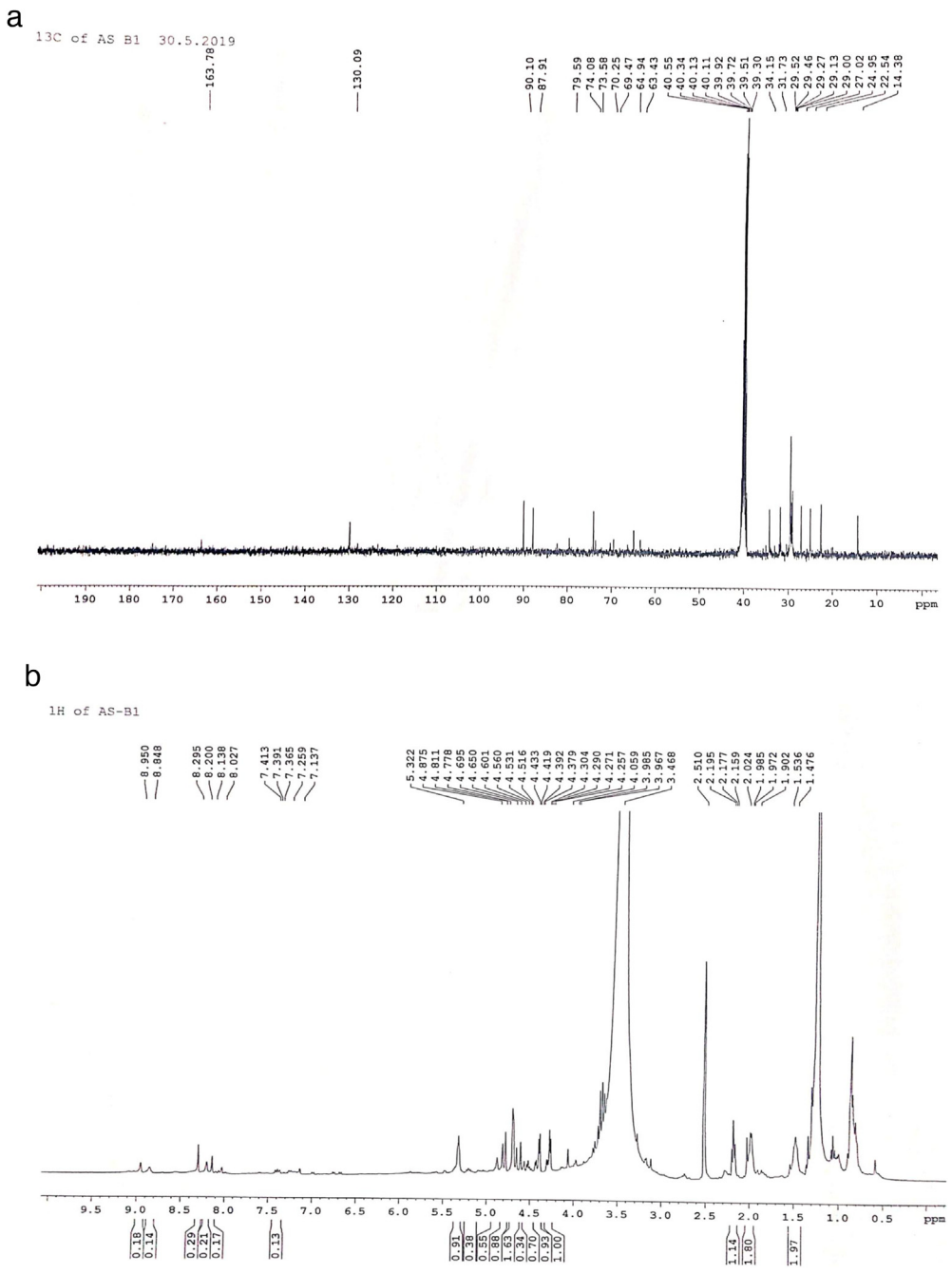

Fig. 6. a The ^{13}C nuclear magnetic resonance spectrum for the purified pigment fraction of the major band. b The ^{1}H nuclear magnetic resonance spectrum for the purified pigment fraction of the major band.

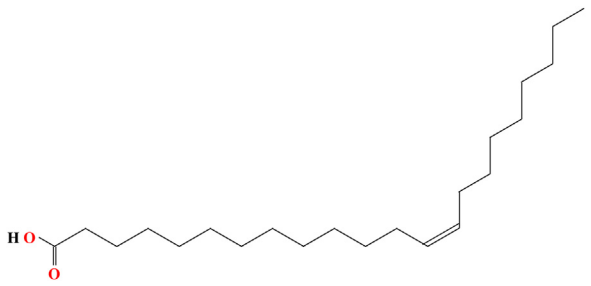

Fig. 7. Structure of erucic acid obtained as the major product after purification from pigment produced by isolated strain BPW19.

include plants of *Brassicaceae* family, particularly rapeseed and mustard. Since plants have higher generation time, industrial use of erucic acid from plants would exhaust the inflow of chief substrates thereby increasing the overall cost of the production system. Plant source for erucic acid also involves other factors like labor cost, seasonality, and large cultivable land. Hence the bacterial source of the compound makes it a significant alternative to avoid the limitations. Apart from these, industrial bacterial culture minimizes the cost of pre-processing, unlike plants that require intermediate steps of chopping, processing, and filtration for the extraction of the compound thus reducing the overall cost. The pigment produced alongside in the bacterial source also serves as a beneficial and commercial by-product.

5. Conclusion

The BPW19 strain was successfully isolated from wastewater and was found to be a member of the *Paenibacillaceae* family. The strain showed psychrotolerant nature, implying its ability to grow both in low and moderate temperature. Since low temperature operations are costlier and are difficult to maintain, giving priority to this fact, the biomass production was optimized at moderate temperature to ensure the ease of the operation. The intercellular bacterial pigment was successfully extracted by sonication assisted solvent extraction using slightly polar solvent indicating the amphiphobic nature of the crude pigment. The crude pigment exhibited antibacterial activity especially against different gram negative bacterial strain enlightening its probable application as an antibacterial substance. The GC-MS analysis detected four major compounds in the crude pigment, namely, dotriacontane; 3,7 dimethyl 7 octanal; 1-eicosene and erucic acid. After column chromatography, the crude pigment was purified and the purified compound was detected as erucic acid by NMR analysis. Erucic acid has many applications in the oleochemical, metallurgical, and automobile industries. This study has established BPW19 as a cost-effective source of a bacterial pigment that may have diverse industrial applications and large scale production of the pigment with optimization and cost efficiency calculation can open up new opportunities for commercialization of the pigment.

Declaration of Competing Interest

The authors report no declarations of interest.

Acknowledgment

The authors would like to acknowledge the National Institute of Technology Rourkela for providing a suitable research environment and the required technical facilities.

Appendix A. Supplementary data

Supplementary material related to this article can be found, in the online version, at doi:https://doi.org/10.1016/j.btre.2021.e00592.

References

[1] M. Sabet, M. Salavati-Niasari, O. Amiri, Using different chemical methods for deposition of CdS on TiO_2 surface and investigation of their influences on the dye-sensitized solar cell performance, Electrochim. Acta 117 (2014) 504–520, doi:http://dx.doi.org/10.1016/j.electacta.2013.11.176.

[2] G. Bisht, S. Srivastava, R. Kulshreshtha, A. Sourirajan, D.J. Baulmer, K. Dev, Applications of red pigments from psychrophilic *Rhodonellum psychrophilum* GL8 in health, food and antimicrobial finishes on textiles, Process Biochem. 94 (2020) 15–29, doi:http://dx.doi.org/10.1016/j.procbio.2020.03.021.

[3] Dyes and pigments market size, Share & Trends Analysis Report by Product (dyes (reactive, Vat, Acid, Direct, Disperse), Pigment (organic, Inorganic)), by Application, by Region, and Segment Forecasts, 2020 – 2027, Market Report Analysis, (2020) Report ID: GVR-1-68038-545-548. Accessed 24 August 2020.

[4] P. Bakthavachalu, S.M. Kannan, M.W. Qoronfleh, Food color and autism: a meta-analysis, in: M.M. Essa, M.W. Qoronfleh (Eds.), Personalized Food Intervention and Therapy for Autism spectrum Disorder Management, Springer, Cham, 2020, pp. 481–504, doi:http://dx.doi.org/10.1007/978-3-030-30402-7.

[5] A. Tkaczyk, K. Mitrowska, A. Posyniak, Synthetic organic dyes as contaminants of the aquatic environment and their implications for ecosystems: a review, Sci. Total Environ. 717 (2020)137222, doi:http://dx.doi.org/10.1016/j.scitotenv.2020.137222.

[6] Y. Orooji, M. Ghanbari, O. Amiri, M. Salavati-Niasari, Facile fabrication of silver iodide/graphitic carbon nitride nanocomposites by notable photo-catalytic performance through sunlight and antimicrobial activity, J. Hazard. Mater. 389 (2020)122079, doi:http://dx.doi.org/10.1016/j.jhazmat.2020.122079.

[7] M.H. Khorasanizadeh, R. Monsef, O. Amiri, M. Amiri, M. Salavati-Niasari, Sonochemical-assisted route for synthesis of spherical shaped holmium vanadate nanocatalyst for polluted waste water treatment, Ultrason. Sonochem. 58 (2019)104686, doi:http://dx.doi.org/10.1016/j.ultsonch.2019.104686.

[8] A.J. Sisi, M. Fathinia, A. Khataee, Y. Orooji, Systematic activation of potassium peroxydisulfate with ZIF-8 via sono-assisted catalytic process: mechanism and ecotoxicological analysis, J. Mol. Liq. 308 (2020)113018, doi:http://dx.doi.org/10.1016/j.molliq.2020.113018.

[9] M. Salavati-Niasari, D. Ghanbari, M.R. Loghman-Estarki, Star-shaped PbS nanocrystals prepared by hydrothermal process in the presence of thioglycolic acid, Polyhedron 35 (2012) 149–153, doi:http://dx.doi.org/10.1016/j.poly.2012.01.010.

[10] P. Mehdizadeh, Y. Orooji, O. Amiri, M. Salavati-Niasari, H. Moayedi, Green synthesis using cherry and orange juice and characterization of $TbFeO_3$ ceramic nanostructures and their application as photocatalysts under UV light for removal of organic dyes in water, J. Clean. Prod. 252 (2020)119765, doi:http://dx.doi.org/10.1016/j.jclepro.2019.119765.

[11] M. Dastkhoon, M. Ghaedi, A. Asfaram, R. Jannesar, F. Sadeghfar, Magnetic based nanocomposite sorbent combination with ultrasound assisted for solid-phase microextraction of Azure II in water samples prior to its determination spectrophotometric, J. Colloid Interface Sci. 513 (2018) 240–250, doi:http://dx.doi.org/10.1016/j.jcis.2017.11.031.

[12] A. Asfaram, M. Ghaedi, H. Javadian, A. Goudarzi, Cu- and S- @SnO_2 nanoparticles loaded on activated carbon for efficient ultrasound assisted dispersive μSPE-spectrophotometric detection of quercetin in *Nasturtium officinale* extract and fruit juice samples: CCD-RSM design, Ultrason. Sonochem. 47 (2018) 1–9, doi:http://dx.doi.org/10.1016/j.ultsonch.2018.04.008.

[13] M. Salavati-Niasari, Synthesis and characterization of host (nanodimensional pores of zeolite-Y)–guest [unsaturated 16-membered Octaaza–macrocycle Manganese(II), Cobalt(II), Nickel(II), Copper(II), and Zinc(II) complexes] nanocomposite Materials, Chem. Lett. 34 (2005) 1444–1445, doi:http://dx.doi.org/10.1246/cl.2005.1444.

[14] M. Ghasemi, A. Khataee, P. Gholami, R. Soltani, A. Hassani, Y. Orooji, In-situ electro-generation and activation of hydrogen peroxide using a CuFeNLDH-CNTs modified graphite cathode for degradation of cefazolin, J. Environ. Manage. 267 (2020)110629, doi:http://dx.doi.org/10.1016/j.jenvman.2020.110629.

[15] R. Monsef, M. Ghiyasiyan-Arani, M. Salavati-Niasari, Application of ultrasound-aided method for the synthesis of $NdVO_4$ nano-photocatalyst and investigation of eliminate dye in contaminant water, Ultrason. Sonochem. 42 (2018) 201–211, doi:http://dx.doi.org/10.1016/j.ultsonch.2017.11.025.

[16] Y. Orooji, R. Mohassel, O. Amiri, A. Sobhani, M. Salavati-Niasari, Gd_2ZnMnO_6/ZnO nanocomposites: green sol-gel auto-combustion synthesis, characterization and photocatalytic degradation of different dye pollutants in water, J. Alloys Compd. 835 (2020)155240, doi:http://dx.doi.org/10.1016/j.jallcom.2020.155240.

[17] R. Monsef, M. Ghiyasiyan-Arani, M. Salavati-Niasari, Utilizing of neodymium vanadate nanoparticles as an efficient catalyst to boost the photocatalytic water purification, J. Environ. Manage. 230 (2019) 266–281, doi:http://dx.doi.org/10.1016/j.jenvman.2018.09.080.

[18] F. Davar, M. Salavati-Niasari, Synthesis and characterization of spinel-type zinc aluminate nanoparticles by a modified sol–gel method using new precursor, J. Alloys Compd. 509 (2011) 2487–2492, doi:http://dx.doi.org/10.1016/j.jallcom.2010.11.058.

[19] Y. Orooji, A. Alizadeh, E. Ghasali, M.R. Derakhshandeh, M. Alizadeh, M. Shahedi Asl, T. Ebadzadeh, Co-reinforcing of mullite-TiN-CNT composites with ZrB_2 and TiB_2 compounds, Ceram. Int. 45 (2019) 20844–20854, doi:http://dx.doi.org/10.1016/j.ceramint.2019.07.072.

[20] M. Salavati-Niasari, M. Loghman-Estarki, F. Davar, Controllable synthesis of nanocrystalline CdS with different morphologies by hydrothermal process in the presence of thioglycolic acid, Chem. Eng. J. 145 (2008) 346–350, doi:http://dx.doi.org/10.1016/j.cej.2008.08.040.

[21] F. Mohandes, F. Davar, M. Salavati-Niasari, Magnesium oxide nanocrystals via thermal decomposition of magnesium oxalate, J. Phys. Chem. Solids 71 (2010) 1623–1628, doi:http://dx.doi.org/10.1016/j.jpcs.2010.08.014.

[22] M. Salavati-Niasari, Ship-in-a-bottle synthesis, characterization and catalytic oxidation of styrene by host (nanopores of zeolite-Y)/guest ([bis(2-hydroxyanil)acetylacetonato manganese(III)]) nanocomposite materials (HGNM), Microporous Mesoporous Mater. 95 (2006) 248–256, doi:http://dx.doi.org/10.1016/j.micromeso.2006.05.025.

[23] A. Asfaram, M. Ghaedi, M.K. Purkait, Novel synthesis of nanocomposite for the extraction of Sildenafil Citrate (Viagra) from water and urine samples: process screening and optimization, Ultrason. Sonochem. 38 (2017) 463–472, doi:http://dx.doi.org/10.1016/j.ultsonch.2017.03.045.

[24] A. Asfaram, E. Dil, P. Arabkhani, F. Sadeghfar, M. Ghaedi, Magnetic Cu: CuO-GO nanocomposite for efficient dispersive micro-solid phase extraction of polycyclic aromatic hydrocarbons from vegetable, fruit, and environmental water samples by liquid chromatographic determination, Talanta 218 (2020) 121131, doi:http://dx.doi.org/10.1016/j.talanta.2020.121131.

[25] A. Sarkar, D. Sarkar, K. Poddar, Nanotoxicity: sources and effects on environment, in: R. Prasad (Ed.), Microbial Nanobionics, Springer, Cham, 2019, pp. 169–179, doi:http://dx.doi.org/10.1007/978-3-030-16534-5.

[26] A. Sarkar, D. Sarkar, K. Poddar, Plant metabolites as new leads to drug discovery: approaches and challenges, in: M.K. Swamy, J.K. Patra, G.R. Rudramurthy (Eds.), Medicinal Plants: Chemistry, Pharmacology, and Therapeutic Applications, CRC Press, Boca Raton, 2019, pp. 61–69, doi:http://dx.doi.org/10.1201/9780429259968-5.

[27] N. Gupta, K. Poddar, D. Sarkar, N. Kumari, B. Padhan, A. Sarkar, Fruit waste management by pigment production and utilization of residual as bioadsorbent, J. Environ. Manage. 244 (2019) 138–143, doi:http://dx.doi.org/10.1016/j.jenvman.2019.05.055.
[28] S. Sánchez-Muñoz, G. Mariano-Silva, M.O. Leite, F.B. Mura, M.L. Verma, S.S. da Silva, A.K. Chandel, Production of fungal and bacterial pigments and their applications, in: M.L. Verma, A.K. Chandel (Eds.), Biotechnological Production of Bioactive Compounds, Elsevier, 2020, pp. 327–361, doi:http://dx.doi.org/10.1016/C2018-0-02574-8.
[29] E. Setiyono, T.H.P. Brotosudarmo, D. Pringgenies, M.N.U. Prihastyanti, Y. Shioi, Analysis of β-cryptoxanthin from yellow pigmented marine bacterium *erythrobacter* sp. kj5, IOP Conf. Ser. Earth Environ. Sci, 246(2019) 012004.
[30] S. PB, A. JC, J. Rathinamala, S. Jayashree, The role of red pigment prodigiosin from bacteria of earthworm gut as an anticancer agent, J. Microbiol. Biotechnol. Food Sci. 4 (2019) 246–251, doi:http://dx.doi.org/10.15414/jmbfs.2014-15.4.3.246-251.
[31] S. DeBritto, T.D. Gajbar, P. Satapute, L. Sundaram, R.Y. Lakshmikantha, S. Jogaiah, S.I. Ito, Isolation and characterization of nutrient dependent pyocyanin from *Pseudomonas aeruginosa* and its dye and agrochemical properties, Sci. Rep. 10 (2020) 1–12, doi:http://dx.doi.org/10.1038/s41598-020-58335-6.
[32] N.E.A. El-Naggar, M.H. Hussein, A.A. El-Sawah, Bio-fabrication of silver nanoparticles by phycocyanin, characterization, in vitro anticancer activity against breast cancer cell line and in vivo cytotoxicity, Sci. Rep. 7 (2017)10844, doi:http://dx.doi.org/10.1038/s41598-017-11121-3.
[33] P. Hernández-Velasco, I. Morales-Atilano, M. Rodríguez-Delgado, J.M. Rodríguez-Delgado, D. Luna-Moreno, F.G. Ávalos-Alanís, J.F. Villarreal-Chiu, Photoelectric evaluation of dye-sensitized solar cells based on prodigiosin pigment derived from *Serratia marcescens* 11E, Dye. Pigment. 177 (2020) 108278, doi:http://dx.doi.org/10.1016/j.dyepig.2020.108278.
[34] F.A. Venegas, G. Köllisch, K. Mark, W.E. Diederich, A. Kaufmann, S. Bauer, M. Chavarría, J.J. Araya, A.J. García-Piñeres, The bacterial product violacein exerts an immunostimulatory effect via TLR8, Sci. Rep. 9 (2019) 1–17, doi:http://dx.doi.org/10.1038/s41598-019-50038-x.
[35] C.K. Venil, Z.A. Zakaria, W.A. Ahmad, Optimization of culture conditions for flexirubin production by *Chryseobacterium artocarpi* CECT 8497 using response surface methodology, Acta Biochim. Pol. 62 (2015) 185–190.
[36] M. Assia, A. Hasnaa, M. Sara, M. Jamal, M. Mohammed, Physico-chemical characterization of a pink red-like pigments produced by five new bacterial soil strains identified as *Streptomyces coelicoflavus*, Am. J. Microbiol. Res. 6 (2018) 67–72, doi:http://dx.doi.org/10.12691/ajmr-6-3-1.
[37] N. Órdenes-Aenishanslins, G. Anziani-Ostuni, M. Vargas-Reyes, J. Alarcón, A. Tello, J.M. Pérez-Donoso, Pigments from UV-resistant Antarctic bacteria as photosensitizers in dye sensitized solar cells, J. Photochem. Photobiol. B 162 (2016) 707–714, doi:http://dx.doi.org/10.1016/j.jphotobiol.2016.08.004.
[38] D. Asker, Isolation and characterization of a novel, highly selective astaxanthin- producing marine bacterium, J. Agric. Food Chem. 65 (2017) 9101–9109, doi:http://dx.doi.org/10.1021/acs.jafc.7b03556.
[39] T. Kimura, W. Fukuda, T. Sanada, T. Imanaka, Characterization of water-soluble dark- brown pigment from Antarctic bacterium, *Lysobacter oligotrophicus*, J. Biosci. Bioeng. 120 (2015) 58–61, doi:http://dx.doi.org/10.1016/j.jbiosc.2014.11.020.
[40] P.S. Selvi, P. Iyer, Isolation and characterization of pigments from marine soil microorganisms, IJLSSR 4 (2018) 2003–2011, doi:http://dx.doi.org/10.21276/ijlssr.2018.4.5.7.
[41] S. Finger, F.A. Godoy, G. Wittwer, C.P. Aranda, R. Calderón, C.D. Miranda, Purification and characterization of indochrome type blue pigment produced by *Pseudarthrobacter* sp. 34LCH1 isolated from Atacama desert, J. Ind. Microbiol. Biot. 46 (2019) 101–111, doi:http://dx.doi.org/10.1007/s10295-018-2088-3.
[42] T.R. Silva, R. Canela-Garayoa, J. Eras, M.V. Rodrigues, F.N. dos Santos, M.N. Eberlin, I.A. Neri-Numa, G.M. Pastore, R.S. Tavares, H.M. Debonsi, L.R. Cordeiro, Pigments in an iridescent bacterium, *Cellulophaga fucicola*, isolated from Antarctica, Antonie Van Leeuwenhoek 112 (2019) 479–490, doi:http://dx.doi.org/10.1007/s10482-018-1179-5.
[43] D. Sarkar, S. Prajapati, K. Poddar, A. Sarkar, Production of ethanol by *Enterobacter* sp. EtK3 during fruit waste biotransformation, Int. Biodeterior. Biodegrad. 145 (2019)104795, doi:http://dx.doi.org/10.1016/j.ibiod.2019.104795.
[44] B. Ramola, V. Kumar, M. Nanda, Y. Mishra, T. Tyagi, A. Gupta, N. Sharma, Evaluation, comparison of different solvent extraction, cell disruption methods and hydrothermal liquefaction of *Oedogonium* macroalgae for biofuel production, Biotechnol. Rep. 22 (2019), doi:http://dx.doi.org/10.1016/j.btre.2019.e00340 e00340.
[45] M.A. Dar, A.A. Shaikh, K.D. Pawar, R.S. Pandit, Exploring the gut of *Helicoverpa armigera* for cellulose degrading bacteria and evaluation of a potential strain for lignocellulosic biomass deconstruction, Process Biochem. 73 (2018) 142–153, doi:http://dx.doi.org/10.1016/j.procbio.2018.08.001.
[46] D. Sarkar, K. Gupta, K. Poddar, R. Biswas, A. Sarkar, Direct conversion of fruit waste to ethanol using marine bacterial strain *Citrobacter* sp. E4, Process Saf. Environ. 128 (2019) 203–210, doi:http://dx.doi.org/10.1016/j.psep.2019.05.051.
[47] K. Poddar, D. Sarkar, A. Sarkar, Construction of potential bacterial consortia for efficient hydrocarbon degradation, Int. Biodeterior. Biodegrad. 144 (2019) 104770, doi:http://dx.doi.org/10.1016/j.ibiod.2019.104770.
[48] B.Y. Gül, I. Koyuncu, Assessment of new environmental quorum quenching bacteria as a solution for membrane biofouling, Process Biochem. 61 (2017) 137–146, doi:http://dx.doi.org/10.1016/j.procbio.2017.05.030.
[49] E. Vila, D. Hornero-Méndez, G. Azziz, C. Lareo, V. Saravia, Carotenoids from heterotrophic bacteria isolated from Fildes Peninsula, King George Island, Antarctica, Biotechnol. Rep. 21 (2019), doi:http://dx.doi.org/10.1016/j.btre.2019.e00306 e00306.
[50] U. Dey, S. Chatterjee, N.K. Mondal, Isolation and characterization of arsenic-resistant bacteria and possible application in bioremediation, Biotechnol. Rep. 10 (2016) 1–7, doi:http://dx.doi.org/10.1016/j.btre.2016.02.002.
[51] I. Kim, J. Kim, G. Chhetri, T. Seo, *Flavobacterium humi* sp. nov., a flexirubin-type pigment producing bacterium, isolated from soil, J. Microbiol. 57 (2019) 1079–1085, doi:http://dx.doi.org/10.1016/j.procbio.2017.05.003.
[52] B. Biswas, B. Sarkar, S. McClure, R. Naidu, Modified osmium tracer technique enables precise microscopic delineation of hydrocarbon-degrading bacteria in clay aggregates, Environ. Technol. Innov. 7 (2017) 12–20, doi:http://dx.doi.org/10.1016/j.eti.2016.11.002.
[53] N.M. Elkenawy, A.S. Yassin, H.N. Elhifnawy, M.A. Amin, Optimization of prodigiosin production by *Serratia marcescens* using crude glycerol and enhancing production using gamma radiation, Biotechnol. Rep. 14 (2017) 47–53, doi:http://dx.doi.org/10.1016/j.btre.2017.04.001.
[54] P. Kaur, G. Ghoshal, A. Jain, Bio-utilization of fruits and vegetables waste to produce β-carotene in solid-state fermentation: characterization and antioxidant activity, Process Biochem. 76 (2019) 155–164, doi:http://dx.doi.org/10.1016/j.procbio.2018.10.007.
[55] D. Sarkar, S. Prajapati, K. Poddar, A. Sarkar, Ethanol production by *Klebsiella* sp. SWET4 using banana peel as feasible substrate, Biomass Convers. Biorefin. (2020) 1–13, doi:http://dx.doi.org/10.1007/s13399-020-00880-1.
[56] G. Sharmila, C. Muthukumaran, E. Suriya, R.M. Keerthana, M. Kamatchi, N.M. Kumar, T. Anbarasan, J. Jeyanthi, Ultrasound aided extraction of yellow pigment from *Tecoma castanifolia* floral petals: optimization by response surface method and evaluation of the antioxidant activity, Ind. Crops Prod. 130 (2019) 467–477, doi:http://dx.doi.org/10.1016/j.indcrop.2019.01.008.
[57] J.W. Choi, J.P. Park, Water-soluble red pigment production by *Paecilomyces sinclairii* and biological characterization, Biotechnol. Bioprocess Eng. 23 (2018) 246–249, doi:http://dx.doi.org/10.1007/s12257-018-0103-1.
[58] F. Meddeb-Mouelhi, J.K. Moisan, J. Bergeron, B. Daoust, M. Beauregard, Structural characterization of a novel antioxidant pigment produced by a photochromogenic *Microbacterium oxydans* strain, Appl. Biochem. Biotechnol. 180 (2016) 1286–1300, doi:http://dx.doi.org/10.1007/s12010-016-2167-8.
[59] S.S. Narayani, S. Saravanan, S. Bharathiaraja, S. Mahendran, Extraction, partially purification and study on antioxidant property of fucoxanthin from *Sargassum cinereum* J. Agardh, J. Chem. Pharm. Res. 8 (2016) 610–616.
[60] S.S. Kharade, K.C. Samal, G.R. Rout, High performance thin layer chromatography fingerprint profile of rhizome extracts of five important *Curcuma* species, Proc. Natl. Acad. Sci. India Sect. B Biol. Sci. 87 (2017) 1335–1341, doi:http://dx.doi.org/10.1007/s40011-016-0709-z.
[61] G. Mukherjee, S.K. Singh, Purification and characterization of a new red pigment from *Monascus purpureus* in submerged fermentation, Process Biochem. 46 (2011) 188–192, doi:http://dx.doi.org/10.1016/j.procbio.2010.08.006.
[62] M. Numan, S. Bashir, R. Mumtaz, S. Tayyab, I. Ullah, A.L. Khan, Z.K. Shinwari, A. Al-Harrasi, Chemical profile and in-vitro pharmacological activities of yellow pigment extracted from *Arthrobacter gandavensis*, Process Biochem. 75 (2018) 74–82, doi:http://dx.doi.org/10.1016/j.procbio.2018.08.033.
[63] G. Mohan, A.K.T. Thangappanpillai, B. Ramasamy, Antimicrobial activities of secondary metabolites and phylogenetic study of sponge endosymbiotic bacteria, *Bacillus* sp. at Agatti Island, Lakshadweep Archipelago, Biotechnol. Rep. 11 (2016) 44–52, doi:http://dx.doi.org/10.1016/j.btre.2016.06.001.
[64] L. Zhou, T. Zhang, S. Tang, X. Fu, S. Yu, Pan-genome analysis of *Paenibacillus polymyxa* strains reveals the mechanism of plant growth promotion and biocontrol, Antonie Van Leeuwenhoek (2020) 1–20.
[65] M. Wu, Y. Zong, W. Guo, G. Wang, M. Li, *Paenibacillus montanisoli* sp. nov., isolated from mountain area soil, Int. J. Syst. Evol. Microbiol. 68 (2018) 3569–3575, doi:http://dx.doi.org/10.1099/ijsem.0.003036.
[66] I.V. Yegorenkova, K.V. Tregubova, A.V. Schelud'ko, Motility in liquid and semisolid media of *Paenibacillus polymyxa* associative rhizobacteria differing in exopolysaccharide yield and properties, Symbiosis 74 (2018) 31–42, doi:http://dx.doi.org/10.1007/s13199-017-0492-5.
[67] C.I. Lo, S.A. Sankar, B. Fall, B. Sambe-Ba, O. Mediannikov, C. Robert, N. Faye, B. Wade, D. Raoult, P.E. Fournier, F. Fenollar, High-quality genome sequence and description of *Paenibacillus dakarensis* sp. nov, New Microbes New Infect. 10 (2016) 132–141, doi:http://dx.doi.org/10.1016/j.nmni.2016.01.011.
[68] S. Huecas, A.J. Canosa-Valls, L. Araújo-Bazán, F.M. Ruiz, D.V. Laurents, C. Fernández-Tornero, J.M. Andreu, Nucleotide-induced folding of cell division protein FtsZ from *Staphylococcus aureus*, FEBS J. (2020), doi:http://dx.doi.org/10.1111/febs.15235.
[69] A.S. Panwar, D. Molpa, G.K. Joshi, Biotechnological potential of some cold-adapted bacteria isolated from North-Western Himalaya, Microbiology 88 (2019) 343–352, doi:http://dx.doi.org/10.1134/S002626171903007X.
[70] H. Kim, A.K. Park, J.H. Lee, S.C. Shin, H. Park, H.W. Kim, PsEst3, a new psychrophilic esterase from the Arctic bacterium *Paenibacillus* sp. R4: crystallization and X-ray crystallographic analysis, Acta Crystallogr. F 74 (2018) 367–372, doi:http://dx.doi.org/10.1107/S2053230X18007525.
[71] M. Helmond, M.N.N. Groot, H. van Bokhorst-van de Veen, Characterization of four *Paenibacillus* species isolated from pasteurized, chilled ready-to-eat meals, Int. J. Food Microbiol. 252 (2017) 35–41, doi:http://dx.doi.org/10.1016/j.ijfoodmicro.2017.04.008.

[72] S.H. Park, W. Yoo, C.W. Lee, C.S. Jeong, S.C. Shin, H.W. Kim, H. Park, K.K. Kim, T.D. Kim, J.H. Lee, Crystal structure and functional characterization of a cold-active acetyl xylan esterase (PbAcE) from psychrophilic soil microbe *Paenibacillus* sp, PLoS One 13 (2018), doi:http://dx.doi.org/10.1371/journal.pone.0206260.
[73] Understanding Temperature Control in Bioreactor Systems, Thermal Stability in Bioreactors, Process Worldwide, 2021 Accessed 24 April 2020.
[74] E. Maleki, Psychrophilic anaerobic membrane bioreactor (AnMBR) for treating malting plant wastewater and energy recovery, J. Water Process Eng. 34 (2020) 101174, doi:http://dx.doi.org/10.1016/j.jwpe.2020.101174.
[75] D. Rettori, N. Durán, Production, extraction and purification of violacein: an antibiotic pigment produced by *Chromobacterium violaceum*, World J. Microbiol. Biotechnol. 14 (1998) 685–688, doi:http://dx.doi.org/10.1023/A:1008809504504.
[76] M.T. Sibero, T.U. Bachtiarini, A. Trianto, A.H. Lupita, D.P. Sari, Y. Igarashi, E. Harunari, A.R. Sharma, O.K. Radjasa, A. Sabdono, Characterization of a yellow pigmented coral-associated bacterium exhibiting anti-bacterial activity against multidrug resistant (MDR) organism, Egypt. J. Aquat. Res. 45 (2019) 81–87, doi:http://dx.doi.org/10.1016/j.ejar.2018.11.007.
[77] S. Afra, A. Makhdoumi, M.M. Matin, J. Feizy, A novel red pigment from marine *Arthrobacter* sp. G20 with specific anticancer activity, J. Appl. Microbiol. 123 (2017) 1228–1236, doi:http://dx.doi.org/10.1111/jam.13576.
[78] D. Alem, J.J. Marizcurrena, V. Saravia, D. Davyt, W. Martinez-Lopez, S. Castro-Sowinski, Production and antiproliferative effect of violacein, a purple pigment produced by an Antarctic bacterial isolate, World J. Microbiol. Biotechnol. 36 (2020), doi:http://dx.doi.org/10.1007/s11274-020-02893-4.
[79] S.Y. Choi, S. Kim, S. Lyuck, S.B. Kim, R.J. Mitchell, High-level production of violacein by the newly isolated *Duganella violaceinigra* str. NI28 and its impact on *Staphylococcus aureus*, Sci. Rep. 5 (2015), doi:http://dx.doi.org/10.1038/srep15598.
[80] B. Khanam, R. Chandra, Comparative analysis of prodigiosin isolated from endophyte *Serratia marcescens*, Lett. Appl. Microbiol. 66 (2018) 194–201, doi:http://dx.doi.org/10.1111/lam.12840.
[81] E.N. Grady, J. MacDonald, L. Liu, A. Richman, Z.C. Yuan, Current knowledge and perspectives of *Paenibacillus*: a review, Microb. Cell Fact. 15 (2016) 203, doi:http://dx.doi.org/10.1186/s12934-016-0603-7.
[82] K. Zorn, I. Oroz-Guinea, U.T. Bornscheuer, Strategies for enriching erucic acid from *Crambe abyssinica* oil by improved *Candida antarctica* lipase A variants, Process Biochem. 79 (2019) 65–73, doi:http://dx.doi.org/10.1016/j.procbio.2018.12.022.
[83] P. Maheshwari, I. Kovalchuk, Genetic transformation of crops for oil production, in: T. McKeon, D. Hayes, D. Hildebrand, R. Weselake (Eds.), Industrial Oil Crops, Academic Press, AOCS Press, 2016, pp. 379–412, doi:http://dx.doi.org/10.1016/B978-1-893997-98-1.00014-2.
[84] R. Katna, M. Suhaib, N. Agrawal, Nonedible vegetable oil-based cutting fluids for machining processes–a review, Mater. Manuf. Process. 35 (2020) 1–32, doi:http://dx.doi.org/10.1080/10426914.2019.1697446.
[88] R. Sowmya, N.M. Sachindra, Carotenoid production by *Formosa* sp. KMW, a marine bacteria of Flavobacteriaceae family: Influence of culture conditions and nutrient composition, Biocatal. Agric. Biotechnol. 4 (2015) 559–567, doi:http://dx.doi.org/10.1016/j.bcab.2015.08.018.